

# Microscopic Nuclear Level Densities from Fe to Ge by the Shell Model Monte Carlo Method

H. Nakada<sup>1</sup> and Y. Alhassid<sup>2</sup>

<sup>1</sup>*Department of Physics, Chiba University, Inage, Chiba 263-8522, Japan*

<sup>2</sup>*Center for Theoretical Physics, Sloane Physics Laboratory, Yale University, New Haven, Connecticut 06520, U.S.A.*

(September 26, 2018)

## Abstract

We calculate microscopically total and parity-projected level densities for  $\beta$ -stable even-even nuclei between Fe and Ge, using the shell model Monte Carlo methods in the complete  $(pf + 0g_{9/2})$ -shell. A single-particle level density parameter  $a$  and backshift parameter  $\Delta$  are extracted by fitting the calculated densities to a backshifted Bethe formula, and their systematics are studied across the region. Shell effects are observed in  $\Delta$  for nuclei with  $Z = 28$  or  $N = 28$  and in the behavior of  $A/a$  as a function of the number of neutrons. We find a significant parity-dependence of the level densities for nuclei with  $A \lesssim 60$ , which diminishes as  $A$  increases.

arXiv:nucl-th/9809066v1 22 Sep 1998

Nuclear level densities are important in theoretical estimates of various compound nuclear reactions. For example, neutron-capture reaction rates are approximately proportional to the corresponding level densities in the neutron resonance region. Neutron capture rates are relevant to the  $s$ - and  $r$ -processes in nucleosynthesis. The  $s$ -process proceeds by a sequence of neutron-capture reactions along the  $\beta$ -stable line, since the  $\beta$ -decay of a radioactive nucleus will occur much faster than the capture of a neutron. The waiting points of the  $r$ -process are determined by the balance between the rates of neutron-capture and of photoejection of a neutron. Accurate methods for calculating level densities are especially useful for nuclei where neutron-capture cross-sections are unavailable experimentally. Nuclei in the iron-group are of special interest since they are the seed nuclei for the synthesis of the heavy elements by the  $s$ - and  $r$ -processes.

Experimentally, level densities are usually extracted from direct counting at low excitation energies ( $E_x \lesssim 5$  MeV), from neutron or proton resonance data [1], from charged particles spectra at intermediate energies ( $5 \lesssim E_x \lesssim 15$  MeV) [2,3], and from Ericson fluctuation analysis at higher energies ( $E_x \gtrsim 15$  MeV) [2]. In many nuclei, the densities at low energies and around the neutron resonance region are well-fitted to phenomenological modifications of the Fermi gas model [4], in particular to the backshifted Bethe formula (BBF) [5,6]. However, the fitted single-particle level density parameter  $a$  and backshift parameter  $\Delta$  are nucleus-dependent and difficult to derive theoretically. Consequently, level densities used in nuclear astrophysical studies are based on various empirical formulae for  $a$  and  $\Delta$  [5–8]. Recently we introduced a novel method to calculate microscopically total and parity-projected level densities [9] in the framework of the auxiliary-field Monte Carlo method. The method takes into account exactly correlations due to effective two-body interactions in a finite shell model space. We showed that realistic nuclear level densities can be calculated with good accuracy if a sufficiently large model space is used. In particular, we applied the method to  $^{56}\text{Fe}$  and found the calculated total level density to be in good agreement with the experimental one. We found a significant parity-dependence of the level density, contrary to the common assumption in astrophysics calculations that positive- and negative-parity levels have equal densities around the neutron resonance region. Shell (or subshell) structure affects the parity dependence of level densities, as pointed out already in Ref. [10] for non-interacting fermions. In this letter, we investigate the systematics of the total and parity-projected level densities of  $\beta$ -stable even-even nuclei between Fe and Ge. The calculated level densities are found to be well-described by the BBF. We extract both  $a$  and  $\Delta$  from the microscopic Monte Carlo densities by fitting them to the BBF, and find shell effects in their systematics. The extracted parameters are also compared with empirical values and with experimentally extracted values when available.

Approximate methods to calculate level densities beyond the Fermi gas model were developed in the framework of the spectral averaging theory [11–13]. Level densities for several  $pf$ -shell nuclei were recently calculated [13] by decomposing the level density into a sum of non-interacting level densities convoluted with Gaussians (the Gaussians reflect the effect of interactions). Since Gaussian spreading is justified only above a certain reference energy, the method used in Ref. [13] requires the knowledge of a complete set of levels up to sufficiently high energy. While reasonable agreement with data is found, two parameters, both of which depend on the nucleus under study, were fitted to the level density data: a reference energy and an interaction parameter. In our level density calculations, no adjustable parameters

have been introduced, yet the calculated level densities are in good agreement with the data.

Neutron resonance energies for  $50 \lesssim A \lesssim 70$  nuclei are in the range  $E_x \lesssim 15$  MeV. To include the important excitations in this mass and energy region in a shell model approach, it is necessary to use the full ( $pf + 0g_{9/2}$ ) model space. This model space is too large for conventional diagonalization methods: instead we use the shell model Monte Carlo (SMMC) method [14] in the complete  $pf$ - and  $0g_{9/2}$ -shell. For level density calculations we need to solve the interacting shell model problem at finite temperature. The SMMC, based on an auxiliary-fields representation of the canonical density matrix at finite temperature, is particularly suitable for such calculations. In this letter we discuss only even-even nuclei. Odd- $A$  and odd-odd nuclei will be considered in a future publication. For an appropriately chosen interaction, even-even nuclei are not subject to the Monte Carlo sign problem, and thus their level densities can be calculated more accurately. Except for even-odd effects due to the pairing correlations (which are reflected in the backshift parameter  $\Delta$ ), important features of the level density systematics can already be deduced from the study of even-even nuclei.

We use the isoscalar Hamiltonian discussed in Ref. [9]. The single-particle energies are calculated in a Woods-Saxon potential plus spin-orbit interaction [4]. The two-body residual interaction includes monopole isovector pairing whose strength is determined from experimental odd-even mass differences, and a self-consistent surface-peaked interaction [15]. The latter is expanded in quadrupole, octupole and hexadecupole terms that are appropriately renormalized. The Hamiltonian is uniquely determined for each nucleus by the above procedure, with no adjustable parameters remaining. Our Hamiltonian includes the dominating collective components of realistic effective interactions [16], yet has the advantage that it satisfies the modified sign rule [17], and therefore has a good Monte Carlo sign for even-even nuclei. This enables us to perform accurate Monte Carlo calculations down to temperatures that are low enough to extract reliable ground state energies. The method used to extract the total level density is explained in Ref. [9]. The canonical thermal energy  $\langle H \rangle_\beta$  (at a fixed proton and neutron number) is calculated in SMMC as a function of inverse temperature  $\beta$ , and then integrated to find the canonical partition function  $Z(\beta)$ . The level density  $\rho$  is evaluated in the saddle-point approximation

$$\rho(E) = (2\pi\beta^{-2}C)^{-1/2}e^S, \quad (1)$$

in terms of the canonical entropy  $S(E) = \beta E + \ln Z$  and the heat capacity  $C = -\beta^2 dE/d\beta$ . Here the relation between energy and temperature is determined by the saddle-point condition  $E(\beta) = \langle H \rangle_\beta$ . The parity-dependence of the level density is calculated using the parity-projection method described in Ref. [9].

To compare with experimental data, it is necessary to find  $\rho$  as a function of the excitation energy. It is thus important to determine accurately the ground-state energy  $E_0$ : any error in  $E_0$  will directly affect the value of the backshift parameter. The ground state energy can be obtained from the thermal energy in the limit of zero temperature, i.e.  $E(\beta \rightarrow \infty)$ . Since the auxiliary-fields propagator matrix used in the Monte Carlo method becomes ill-conditioned [18] at large  $\beta$  ( $\gtrsim 5$  MeV $^{-1}$ ), we have to determine the ground state energy from finite  $\beta$  calculations, where the lowest excited states still contribute to the thermal energy. The ground state of even-even nuclei is  $J^P = 0^+$ , while the first excited state of almost all even-even nuclei is  $J^P = 2^+$  with an excitation energy of  $\sim 1$  MeV in the  $50 \lesssim A \lesssim 70$

mass region. For sufficiently low temperatures ( $\beta \gtrsim 2 - 3 \text{ MeV}^{-1}$ ), the main contribution to  $E(\beta) - E_0$  arises from thermal excitation to the  $2_1^+$  state. In the two-state model of  $0_1^+$  and  $2_1^+$ , we have

$$E(\beta) \approx E_0 + \eta E_x(2_1^+), \quad (2)$$

where  $E_x(2_1^+)$  is the excitation energy of the  $2_1^+$  and  $\eta \equiv 1/\{1 + \exp[\beta E_x(2_1^+)]/5\}$  (where the factor 5 accounts for the spin degeneracy of the  $2^+$  state). The ground state energy  $E_0$  can then be extracted by a two-parameter fit of (2) to the large- $\beta$  Monte Carlo data for  $E(\beta)$ . However, in SMMC we can also calculate  $\langle \vec{J}^2 \rangle_\beta$ , the canonical expectation value of  $\vec{J}^2$ , where  $\vec{J}$  is the angular-momentum operator. In the two-state model

$$\langle \vec{J}^2 \rangle_\beta \approx 6\eta. \quad (3)$$

By fitting the Monte Carlo data of  $\langle \vec{J}^2 \rangle_\beta$  to (3), we can first extract  $E_x(2_1^+)$ , and then use this value in (2) to determine the ground state energy  $E_0$  more accurately by a one-parameter fit. In Fig. 1, the extracted values of  $E_0$  are shown for  $^{58}\text{Fe}$  as a function of  $\beta$ . The present procedure gives a stable  $E_0$  value beyond  $\beta = 2.5 \text{ MeV}^{-1}$ . We adopt the  $E_0$  and  $E_x(2_1^+)$  values by averaging the values in the range  $\beta = 2.5$  to  $3 \text{ MeV}^{-1}$ . Our method not only provides a more accurate determination of  $E_0$  but also gives  $E_x(2_1^+)$ , although with less accuracy (typically  $\sim 0.1 - 0.2 \text{ MeV}$ ) than the ground state energy ( $\sim 0.05 \text{ MeV}$ ). In Fig. 2 we compare the calculated excitation energies with the experimental data, and a fairly good agreement is observed. This is another confirmation that our present interaction includes properly the dominating collective features of the realistic nuclear force. We remark that the first observed excited state in  $^{72}\text{Ge}$  is a  $0^+$ , an exception to the usual  $2^+$ . It is not clear whether our present Hamiltonian can reproduce this  $0_2^+$  state. Experimentally, the  $2_1^+$  state lies only  $0.14 \text{ MeV}$  above the  $0_2^+$ . Because of the spin degeneracy factor, the thermal weight of the  $2_1^+$  is still about three times larger than that of  $0_2^+$  for  $\beta = 3 \text{ MeV}^{-1}$ . Hence we can neglect the contribution of this  $0_2^+$  in the above procedure. The reliability of our Hamiltonian was further confirmed by the average energy of the mass quadrupole excitation in  $^{56}\text{Fe}$  [9].

The BBF level density <sup>1</sup> at excitation energy  $E_x$  is given by

$$\rho(E_x) \approx g \frac{\sqrt{\pi}}{24} a^{-\frac{1}{4}} (E_x - \Delta)^{-\frac{5}{4}} e^{2\sqrt{a(E_x - \Delta)}} \quad (4)$$

with  $g = 2$  for the total level density and  $g = 1$  for the parity-projected densities. The SMMC total level densities are well described by (4), and are in good agreement with the level densities that are reconstructed from experimentally determined  $a$  and  $\Delta$ . For example, in Fig. 3 we compare the SMMC total level densities of  $^{60}\text{Ni}$  and  $^{68}\text{Zn}$  with the experimental ones [1,3] and find good agreement, similar to that found in Ref. [9] for the  $^{56}\text{Fe}$  level

---

<sup>1</sup> The density given by Eq. (4) is sometimes referred to in the literature as “state density” where each level with spin  $J$  is weighted by a factor of  $2J + 1$  (to include its magnetic quantum number degeneracy). All densities calculated in this paper are state densities.

density. The calculated parity-projected level densities are also well fitted to the BBF if parity-specific values for  $a$  and  $\Delta$  (denoted by  $a_{\pm}$  and  $\Delta_{\pm}$ ) are used. In general these values differ from those for the total level densities.

We have extracted the level density parameters  $a$  and  $\Delta$  from SMMC level density calculations for a number of  $\beta$ -stable even-even nuclei in the  $50 \lesssim A \lesssim 70$  region:  $^{54-58}\text{Fe}$ ,  $^{58-64}\text{Ni}$ ,  $^{64-70}\text{Zn}$  and  $^{70,72}\text{Ge}$ . In some of the previous analyses of level densities (see e.g. Ref. [7]), a simple empirical function was assumed for the backshift parameter  $\Delta$ , and the single-particle level density parameter  $a$  was then fitted to the experimental data. In Ref. [1] both  $a$  and  $\Delta$  are fitted to the experimental data. Empirical formulae for  $a$  were proposed in Refs. [1,7], but different formulae yield quite different level densities. Furthermore, there still remains a discrepancy between the experimental and the various empirical values of  $a$ . While these empirical approaches describe the global systematics of the level densities through the nuclear periodic table [8], important nuclear structure effects may be overlooked, resulting in inaccurate level densities for at least some of the nuclei. Our present calculations seem to reproduce available experimental densities with good accuracy (typically within a factor of 2) for  $E_x \lesssim 20$  MeV. Consequently, our extracted level density parameters are expected to be more accurate than the empirical ones. Our values for  $a$  and  $\Delta$  are obtained by fitting the BBF to the SMMC results in the energy range  $4 < E_x < 22$  MeV.

Figures 4 and 5 show the calculated values of  $a$  and  $\Delta$ , as well as the parity-dependent ones  $a_{\pm}$  and  $\Delta_{\pm}$ , as a function of  $A$ . Isotopes are connected by dotted lines. For comparison, the values obtained from the empirical formula of Ref. [7] for the total level density parameters are shown by solid lines. Even-odd staggering in  $\Delta$  due to pairing correlations is not observed here since only even-even nuclei are considered. It is interesting to determine whether shell effects can be observed in the level density parameters. Among the nuclei studied,  $^{54}\text{Fe}$  and the Ni isotopes have  $f_{7/2}$ -shell closure for protons ( $Z = 28$ ) or neutrons ( $N = 28$ ), respectively. In the empirical values of the backshift parameter  $\Delta$  of Ref. [7], no shell effects are seen for these nuclei. In contrast, we find enhancement of  $\Delta$  at  $Z = 28$  or  $N = 28$ , both for the total and parity-projected level densities. Except for the  $Z = 28$  or  $N = 28$  nuclei, the present  $\Delta$  values for the total level densities are close to those of Ref. [7]. On the other hand, we do not observe shell effects at  $Z = 28$  or  $N = 28$  in the single-particle level density parameter  $a$ , which increases rather smoothly as a function of  $A$ . Compared with the empirical estimates of Ref. [7], the present values of  $a$  are not very different in the region  $A \lesssim 65$ , but the  $Z$ -dependence within isobars tends to be weaker. For  $A > 65$  our  $a$  values are considerably smaller than those of Ref. [7]. For  $^{68}\text{Zn}$ , for example, we obtain  $a = 7.79$  as compared with the empirical value of  $a = 8.37$  [7]. Our value lies in between the experimental values of  $a = 7.25$  (assuming half the rigid-body moment of inertia) and  $a = 7.97$  (assuming the rigid-body moment of inertia) [1], and is closer to the rigid-body value. We shall return later to the systematics of  $a$ .

We turn next to the parity-dependence of the level densities. For  $A \lesssim 60$  nuclei we observe that the level density parameters are different for positive- and for negative-parity levels; while  $a_+$  is close to  $a$  of the total level density, we find that  $a_-$  is larger than  $a_+$ . As  $A$  increases,  $a_-$  approaches  $a_+$  (and therefore  $a$ ). Similarly, for  $A \lesssim 60$  nuclei  $\Delta_-$  is substantially larger than  $\Delta_+$  and both  $\Delta_{\pm}$  are different from  $\Delta$ . The difference between  $\Delta_+$  and  $\Delta_-$  becomes smaller as  $A$  increases. The observed parity-dependence originates in the subshell structure in this mass region, where negative-parity states in even-even nuclei

are possible only when the  $g_{9/2}$  level is populated. Because of the energy gap between the  $pf$  and  $g_{9/2}$  orbits we expect the negative-parity level density to be lower than the positive-parity level density at low energies. Thus the backshift  $\Delta_-$  should be larger than  $\Delta_+$ . On the other hand, at high excitation energies positive- and negative-parity level densities are approximately equal, as in the Fermi gas model. Therefore, in the low energy region the negative-parity density is expected to rise more quickly as a function of energy <sup>2</sup>, i.e.  $a_- > a_+$ . As  $A$  increases, excitations (especially of neutrons) to the  $g_{9/2}$  orbit become easier, lessening the difference between  $\rho_+$  and  $\rho_-$ . For  $A \gtrsim 65$  we find that the values of  $a_{\pm}$  and  $\Delta_{\pm}$  are close to those of the total level densities.

In the conventional Fermi gas model the single-particle level density parameter  $a$  is predicted to be proportional to  $A$  [4]. To investigate the  $A$ -dependence of  $a$ , it is customary to define the quantity  $K \equiv A/a$ . In the Fermi gas model  $K$  is nearly constant ( $\sim 16$  MeV). In the empirical model of Ref. [7],  $K$  decreases nearly linearly as  $A$  increases within a family of isotopes, i.e. the level density increases more rapidly as a function of  $E_x$  for heavier isotopes. On the other hand, the empirical formula of Ref. [1] (see Eq. (10) of [1]) predicts a gradual increase of  $K$ . In the present microscopic SMMC calculations, we find that  $K$  (for the total level densities) depends smoothly on the neutron number  $N$ , and is almost independent of the proton number  $Z$  as is shown in Fig. 6.  $K \sim 10$  MeV at  $N = 28$ , and decreases towards the middle of the  $N = 28 - 50$  shell to a value of  $\sim 8.5$  MeV. This behavior clarifies the shell systematics of  $a$ . A similar behavior is observed for  $K_+ \equiv A/a_+$ . Although we cannot make definite conclusions because of the large statistical errors,  $K_- \equiv A/a_-$  seems to be roughly constant.

In conclusion, using the shell model Monte Carlo method in the complete ( $pf + 0g_{9/2}$ )-shell, we have calculated microscopically total and parity-projected level densities for  $\beta$ -stable even-even nuclei in the Fe to Ge region. We have studied the systematics and shell effects in both the single-particle level density parameter  $a$  (as well as the parameter  $K = A/a$ ) and the backshift  $\Delta$ . The shell structure observed in  $\Delta$  at  $Z = 28$  or  $N = 28$  and the systematics of  $K$  differ from those given by various empirical formulae.

This work was supported in part by the DOE grant DE-FG-0291-ER-40608, and by the Ministry of Education, Science and Culture of Japan (grant 08740190). Computational cycles were provided by the IBM SP2 at JAERI and Fujitsu VPP500 at RIKEN.

---

<sup>2</sup> Our BBF parametrization of the parity-dependent level densities is valid only for  $E_x \lesssim 20$  MeV. At higher energies  $\rho_+ \simeq \rho_-$  and therefore  $a_+ \simeq a_-$  should hold.

## REFERENCES

- [1] W. Dilg, W. Schantl, H. Vonach and M. Uhl, Nucl. Phys. **A217** (1973) 269.
- [2] J. R. Huizenga, H. K. Vonach, A. A. Katsanos, A. J. Gorski and C. J. Stephan, Phys. Rev. **182** (1969) 1149.
- [3] C. C. Lu, L. C. Vaz, J. R. Huizenga, Nucl. Phys. **A190** (1972) 229.
- [4] A. Bohr and B. R. Mottelson, *Nuclear Structure* vol. 1 (Benjamin, New York, 1969).
- [5] J. A. Holmes, S. E. Woosley, W. A. Fowler and B. A. Zimmerman, Atom. Data and Nucl. Data Tables **18** (1976) 305.
- [6] J. J. Cowan, F.-K. Thielemann and J. W. Truran, Phys. Rep. **208** (1991) 267.
- [7] S. E. Woosley, W. A. Fowler, J. A. Holmes and B. A. Zimmerman, Atom. Data and Nucl. Data Tables **22** (1978) 371.
- [8] T. Rausher, F.-K. Thielemann and K.-L. Kratz, Phys. Rev. C **56** (1997) 1613.
- [9] H. Nakada and Y. Alhassid, Phys. Rev. Lett. **79** (1997) 2939.
- [10] S. M. Grimes, Phys. Rev. C **38** (1988) 2362.
- [11] K. K. Mon and J. B. French, Ann. Phys. (N.Y.) **95** (1975) 90.
- [12] R. Strohmaier and S. M. Grimes, Z. Phys. A **329** (1988) 431.
- [13] V. K. B. Kota and D. Majumdar, Nucl. Phys. A **604** (1996) 129.
- [14] G. H. Lang, C. W. Johnson, S. E. Koonin and W. E. Ormand, Phys. Rev. **C48** (1993) 1518.
- [15] Y. Alhassid, G. F. Bertsch, D. J. Dean and S. E. Koonin, Phys. Rev. Lett. **77** (1996) 1444.
- [16] M. Dufour and A. P. Zuker, Phys. Rev. C **54** (1996) 1641.
- [17] Y. Alhassid, D. J. Dean, S. E. Koonin, G. Lang, and W. E. Ormand, Phys. Rev. Lett. **72** (1994) 613.
- [18] E. Y. Loh Jr. and J. E. Gubernatis, in *Electronic Phase Transitions*, edited by W. Hanke and Yu. V. Kopayev (North Holland, Amsterdam, 1992), p. 177.

## FIGURES

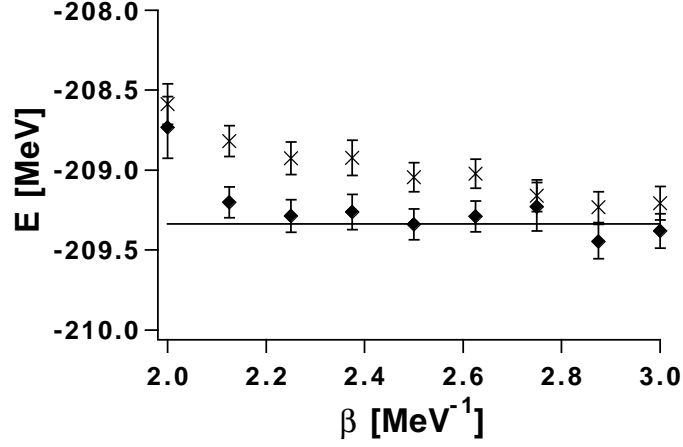


FIG. 1. Thermal energy  $E(\beta)$  in SMMC (crosses) and ground state energy  $E_0$  (diamonds) for  $^{58}\text{Fe}$  extracted via Eqs. (2) and (3). The solid line is the average of the values for  $E_0$  between  $\beta = 2.5$  to  $3 \text{ MeV}^{-1}$ .

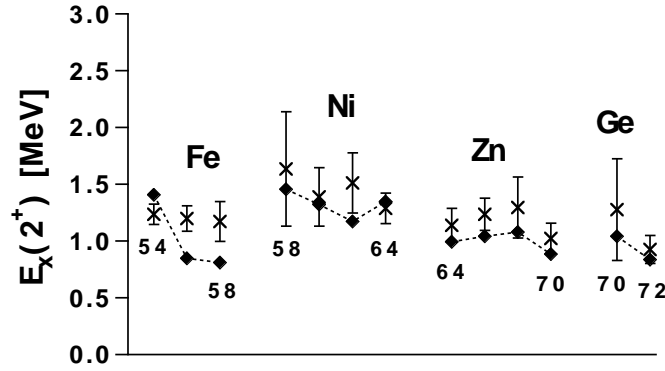


FIG. 2. Excitation energies  $E_x(2^+)$  of the first  $2^+$  state: comparison between the SMMC values (calculated from Eq. (3)) (crosses) and the experimental values (diamonds). Mass numbers are shown for several nuclei below the symbols.



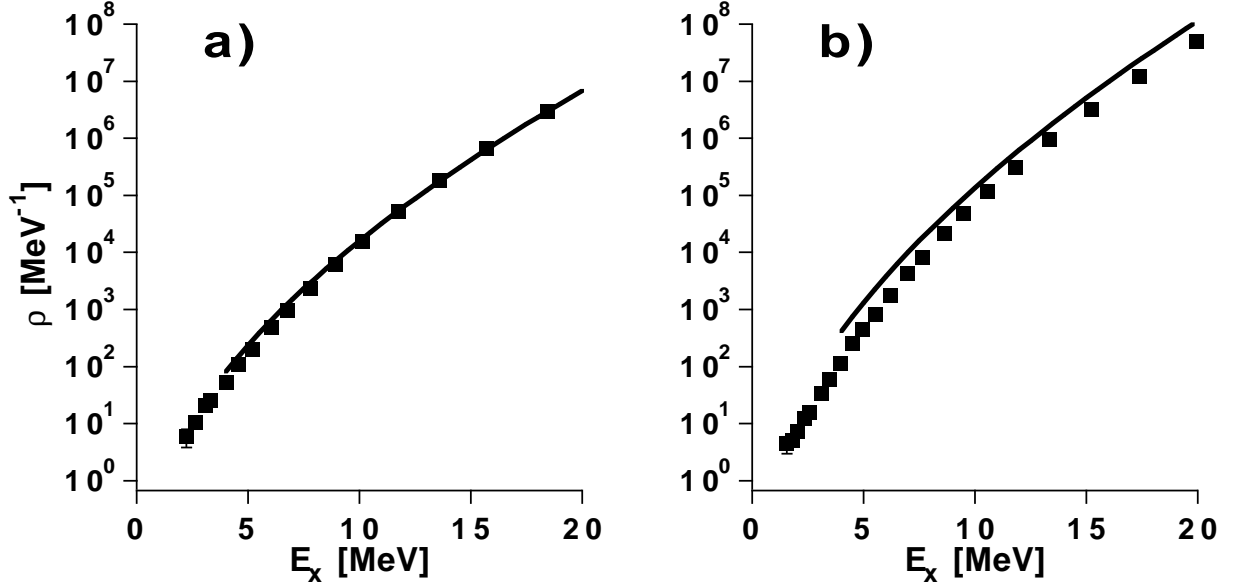


FIG. 3. Total level densities: comparison between SMMC (solid squares with error bars) and experimentally determined level densities (solid lines). a)  $^{60}\text{Ni}$ . The experimental BBF parameters are taken from Ref. [3]. b)  $^{68}\text{Zn}$ . The experimental BBF parameters are taken from Ref. [1] assuming rigid-body moment-of-inertia.

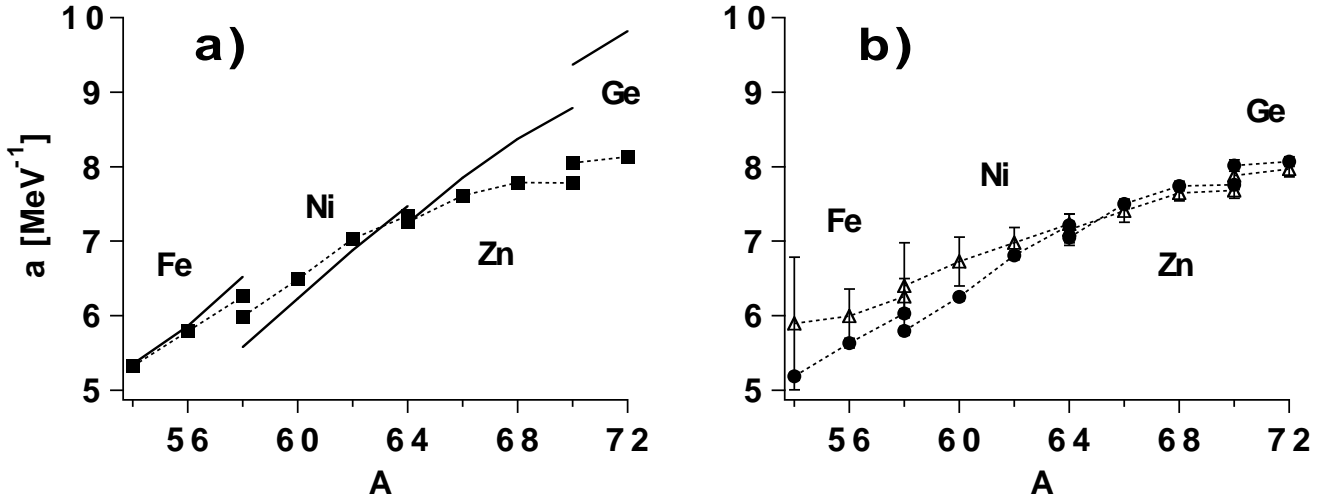


FIG. 4. Single-particle level density parameter  $a$  as a function of  $A$ , obtained from fitting the SMMC level densities to the BBF (4). Isotopes are connected by dotted lines. Left:  $a$  for the total level densities (squares) in comparison with the values obtained from the empirical formula of Ref. [7] (solid lines). Right:  $a_+$  (circles) and  $a_-$  (triangles) of the positive- and negative-parity SMMC level densities, respectively.

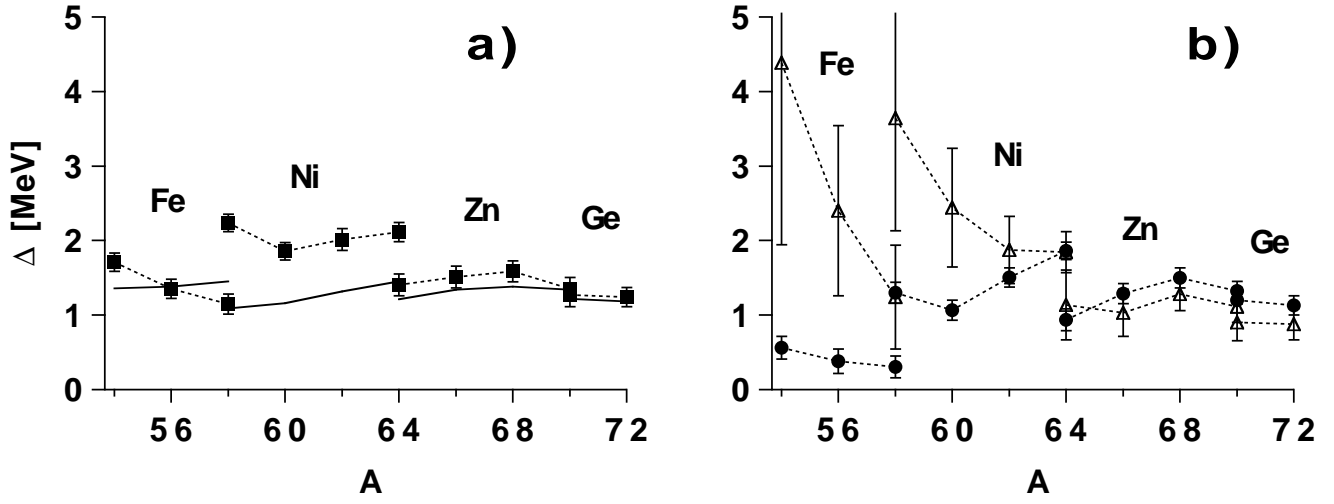


FIG. 5. Backshift parameter  $\Delta$  as a function of  $A$ , obtained from SMMC calculations for total (left) and parity-projected (right) level densities. Conventions are as in Fig. 4.

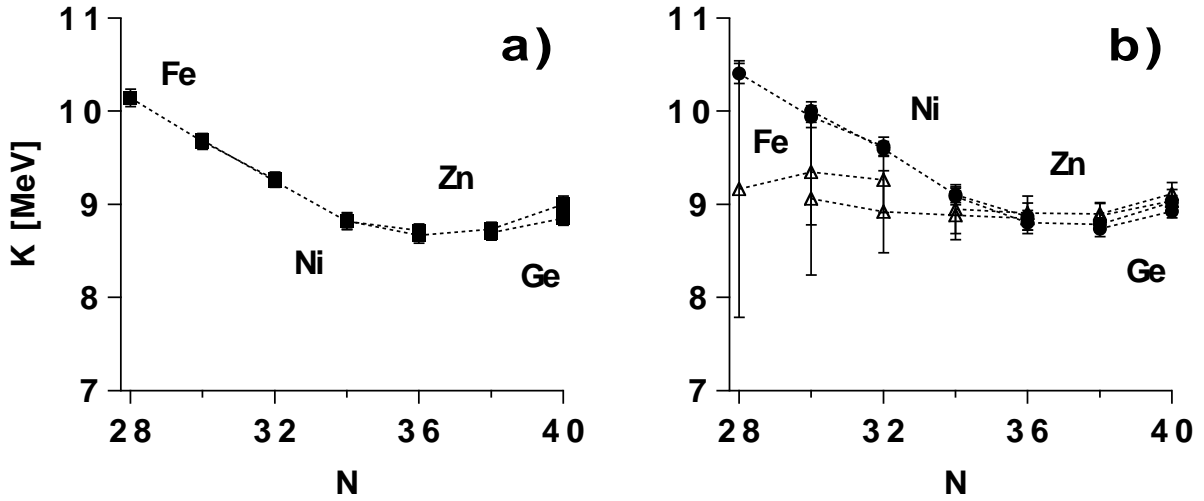


FIG. 6.  $K \equiv A/a$  as a function of neutron number  $N$  from the SMMC calculations for total (left) and parity-projected (right) level densities. Isotopes are connected by dotted lines.